A Computational White Matter Atlas for Aging with Surface-Based Representation of Fasciculi

Hui Zhang[1], Paul A. Yushkevich[1], Daniel Rueckert[2], and James C. Gee[1]

[1] Penn Image Computing and Science Laboratory (PICSL),
Department of Radiology, University of Pennsylvania, Philadelphia, USA
[2] Department of Computing, Imperial College, London, UK

Abstract. Voxel-based analysis, either whole-brain or tract-specific, is a widely used approach for localizing white matter (WM) differences across populations using diffusion tensor imaging (DTI). A prerequisite to this approach is to spatially normalize all the subjects to a common template. The accuracy of spatial normalization can be improved by using a population-specific template that is, morphologically, most similar to the subjects in the population of interest. Here, we report the development of a population-specific DTI template for the elderly using the publicly available IXI brain database. The template captures the average shape and diffusion properties of the aging population and contains segmentations of major WM fasciculi parcellated via fiber tractography. Furthermore, the segmentations are modeled using surface-based representation to support the tract-specific analysis recently proposed by Yushkevich et al. The utility of the template is demonstrated in an examination of WM changes in Amyotrophic Lateral Sclerosis.

1 Introduction

Diffusion tensor imaging (DTI) depicts *in vivo* the intricate architecture of white matter (WM) [1] and has become an indispensable tool for studying WM both in normal populations and in populations with brain disorders. To localize WM differences across populations using DTI, both whole-brain and tract-specific analyses are commonly used [2,3]. A prerequisite to such analyses is spatial normalization which establishes anatomical correspondence among all the subjects in a study, by registering them to some template.

To spatially normalize DTI data, a DTI template is required to leverage recent advances in tensor-based image registration algorithms shown to improve the quality of spatial alignment [4]. Mori et al. has recently developed such a template, known as the ICBM-DTI-81 template [5], which defines the same stereotactic space as the widely used ICBM-152 anatomical template and contains manually-delineated WM regions. The ICBM-DTI-81 template is destined to become an important neuroimaging resource. However, because it is built with healthy controls between 18 and 59 years old, this template does not capture significant morphological changes in brain anatomy for the elderly population (65 years or older). As a result, its application to the aging population may adversely affect the quality of spatial normalization.

B. Fischer, B. Dawant, and C. Lorenz (Eds.): WBIR 2010, LNCS 6204, pp. 83–90, 2010.

In this paper, we report the construction of a population-specific DTI template appropriate for the aging population which, to the best of our knowledge, does not yet exist. To accomodate large morphological variation in anatomy of this population, the template was constructed using a high-dimensional tensor-based image registration method rather than the affine registration method used for creating the ICBM-DTI-81 template. The template construction algorithm also captures simultaneously the average shape and diffusion properties of the population. In addition, a large set of major WM tracts were parcellated using fiber tractography and modeled with the skeleton surface representation to support the tract specific analysis recently developed by Yushkevich et al. [3]. We demonstrated the utility of the template in a study of WM changes in Amyotrophic Lateral Sclerosis (ALS), a devastating, usually fatal, disease of motor neuron degeneration.

The rest of the paper is organized as follows: Sec. 2 gives the imaging and demographic details of the dataset used for building the template, describes the method of template construction, WM tract parcellation and modeling, and discusses the application of the template in ALS. Sec. 3 illustrates the resulting template and the associated skeleton surface models and reports the results from the ALS study. Finally, the paper is summarized in Sec. 4.

2 Materials and Methods

2.1 Subjects and Data Acquisition

The subjects used to construct the proposed aging template are extracted from the IXI brain database (http://www.ixi.org.uk) developed jointly by Imperial College of Science Technology & Medicine and University College London. The IXI database consists of brain MR images from 550 normal subjects between the age of 20 and 80 years that are freely available for downloads. The inclusion criteria for this template construction are 1) subjects are of age 65 years or older; 2) DT-MR images are available and of sufficient quality (i.e., no significant motion or suscepitibility-induced artifacts). A total of 51 subjects, currently determined to meet the selection criteria, have been included in the current paper. The additional qualified subjects will be added in the future. The demographics of the included subjects are age 65-83, mean age and standard deviation 70.4±4.0; 21 males and 30 females. DT-MR data was collected at two sites (Guy's Hospital and Hammersmith Hospital, London, UK) with two different scanners (Philips 1.5 T and 3.0 T) with a single-shot echo-planar diffusion-weighted sequence with 15 non-collinear gradient directions @ b = 1000 s/mm^2 with a SENSE factor of 2. The imaging matrix was 128 x 128 with a field of view 224 x 224 mm^2, resulting in in-plane resolution of 1.75 x 1.75 mm^2. The slice thicknesses are 2.35 mm and 2.0 mm for the two sites, respectively.

2.2 Construction of the Population-Averaged DTI Template

The population-averaged DTI template was constructed using the DT-MR images of all the chosen subjects. We chose the template construction algorithm

described in [4] because the algorithm has been tailored for handling DT-MR images. Briefly, the initial average image is computed as a log-Euclidean mean [6] of the input DT-MR images. The average is then iteratively refined by repeating the following procedure: register the subject images to the current average, then compute a refined average for the next iteration as the mean of the normalized images. This procedure is repeated until the average image converges. The resulting template is unbiased towards any single subject and captures the average diffusion properties of the population at each voxel with a diffusion tensor. Subsequently, the template is "shape-corrected" to ensure that it also represents the average shape of the population, using the strategy proposed by Guimond et al. [7]. This is achieved by first computing an average of the deformation fields that warp each subject into alignment with the template, then warping the template with the inverse of the average deformation field.

In contrast to the ICBM-DTI-81 template that was constructed via affine registration of scalar images derived from diffusion data, the registration algorithm [8] used in the current template construction captures high-dimensional spatial deformations and matches DT-MR images directly. By computing image similarity on the basis of full tensor images, rather than scalar features, the algorithm incorporates local fiber orientations as features to drive the alignment of individual WM tracts. When measuring similarity between tensor images, it is essential to take into account the fact that when a transformation is applied to a tensor field, the orientation of the tensors is changed [9]. A unique property of this registration algorithm is the ability to model the effect of deformation on tensor orientation as an analytic function of the Jacobian matrix of the deformation field. By using full tensor information in the similarity metric, the method aligns WM regions better than scalar-based registration methods, as demonstrated in a task-driven evaluation study [4].

2.3 White Matter Parcellation of the DTI Template

We followed the approach described in [3] and parcellated the DTI template into individual WM tracts using an established protocol by Wakana et al. [10], which is based on fiber tracking. The validity of tracking in a population-averaged DTI template has recently been demonstrated by Lawes et al. [11] in a comparison to classic postmortem dissection. We delineated six major tracts that includes: corpus callosum (CC), corticospinal tracts (CST), inferior fronto-occipital tracts (IFO), inferior longitudinal tracts (ILF), superior longitudinal tracts (SLF), and uncinates (UNC). A common property of these tracts is that all have a major portion that is sheet-like and can be modeled using the surface-based representation as described in Sec. 2.4. White matter tracts that are more appropriately represented by tubular models, such as the tapetum of the CC, the cingulum, the fornix and the optic tract were not segmented. Fasciculi in the cerebellum and brain stem were not considered either. These tubular structures will be included in the future. Only the arcuate portion of the SLF, which can be tracked consistently, was segmented. Binary 3D segmentations of individual tracts were generated by labeling voxels in the DTI template through which at least one fiber

passed. The binary segmentations were further edited using ITK-SNAP [12] to remove extraneous connections.

2.4 Surface-Based Geometric Modeling of WM Tracts

Geometrical modeling of the WM tracts was achieved with the algorithm proposed by Yushkevich et al. [3], which involves fitting deformable medial models (cm-reps) to the binary segmentations derived in Sec. 2.3. The cm-reps are models that describe the skeleton and the boundary of a geometrical object as parametric digital surfaces with predefined topology. The models describe the geometrical relationship between the skeleton and the boundary, such that, during fitting, deformations applied to the model's skeleton can be propagated to the model's boundary.

A key feature of medial models is their ability to parametrize the entire interior of the model using a shape-based coordinate system. This is due to the fact that in medial geometry every point on the skeleton surface is associated with a sphere that is tangent to the boundary surface at a pair of points (which may coincide at edges of the skeleton). The line segments connecting the sphere's center to the points of tangency are called "spokes" and are orthogonal to the boundary. Furthermore, no two spokes intersect inside the model. This allows us to define a coordinate system for interior of the object based entirely on the shape of the object, where two of the coordinate values parametrize the skeleton surface and the third gives the position of a point on the spokes. As shown in [3], in the context of modeling sheet-like WM tracts, this coordinate system affords us the ability to reduce the dimensionality of the problem by projecting data onto the skeleton along the arguably "less interesting" thickness dimension. From the point of view of statistical analysis, this may result in improved sensitivity without much loss in spatial specificity.

2.5 Application to Identify WM Changes in ALS

To demonstrate the utility of the proposed DTI template with surface-based WM modeling, we employed the template to identify WM changes in ALS. The structure-specific statistical mapping described in [3] was used for our analysis, which takes advantage of the surface-based WM models developed as part of our template. Because of the existing hypothesis that ALS strongly affects the motor pathway, only the left and right CSTs were included in the analysis. Briefly, for each subject, its DT-MR image was first registered to the DTI template using the algorithm [8] and warped into the template space. The fitted cm-rep models of the CSTs parcellated in the template were then used to sample the diffusion data in the shape-based coordinate systems established by these models. Specifically, for each location on the skeleton surfaces of the CSTs, the average fractional anisotropy (FA) along its two associated spokes was computed, resulting in an average FA map associated with the skeleton surfaces. After repeating this process for each subject, the original volumetric dataset was dimensionality reduced into a surface dataset. Permutation-based non-parametric suprathreshold cluster analysis was then applied to identify WM differences between the two groups

and the statistics on both CSTs were pooled. The cluster-defining threshold was set at uncorrected p-value = 0.01 and the clusters with FWE-corrected p-value < 0.05 were deemed significant.

The dataset that we chose to analyze were from an earlier ALS study that we have studied [omitted]. It consists of 8 healthy controls and 8 ALS patients. The DT-MR data for these subjects were collected using a 12-direction diffusion imaging protocol on a 3 T Siemens scanner without parallel imaging. In our previous study, we applied the same analysis as here but using a population-specific template built from the subject data alone. We leveraged this earlier result and compared it to the current finding to provide a qualitative assessment of the feasibility of using our proposed template for datasets acquired on different scanners and with different sequences.

3 Results

The population-averaged DTI template is shown in Fig. 1 in terms of its fiber orientation map. Compared to the ICBM-DTI-81 template [5], which is constructed using affine registration, our template has considerably sharper edge features as well as much richer details in the cortical regions. Furthermore, the additional shape-correction step allows our template to capture the average shape of the WM anatomy in the aging population. In particular, observe the distinct asymmetry in the size and shape of the left and right SLFs, with the left SLF (image right) being significantly larger than the right. This is consistent with the known observation that the SLF is larger in the left hemisphere, likely a result of language lateralization [13].

The surface-based geometric modeling of WM tracts is illustrated with Fig. 2 using the left CST as an example. The cm-rep model of the left CST is shown in Panel (c), which consists of a smooth surface patch represented as a triangular mesh and the associated radius function map, which encodes the radius of the sphere at each vertex of the mesh. The boundary surface computed from this model is shown in Panel (d), which is very similar to the binary segmentation of the tract shown in Panel (b), the fitting target. The high-quality of fitting was confirmed quantitatively. Except for the ILF, the Dice overlaps between the binary segmentations and the fitted cm-rep models range from 90% to 95%. The Dice overlap for the ILF is slightly less, around 85%. This is consistent with the results reported in [3], which observed that the poorer fitting of the ILFs is due to the branching near the posterior end of ILF.

The skeleton surfaces of the cm-rep models fitted to all the parcellated tracts are shown in Fig. 3. For the tracts that exist bilaterally, their left and right copies were individually fitted to their corresponding cm-rep models. Hence, the resulting skeleton surfaces reflect the underlying asymmetry in antomy. The asymmetry in the SLFs observed above is evident here as well. Another apparent asymmetry is in the ILFs. However, we believe that this is a result of the intrinsic ambiguity in separating the posterior portion of the ILFs and the IFOs rather than true anatomical ambiguity.

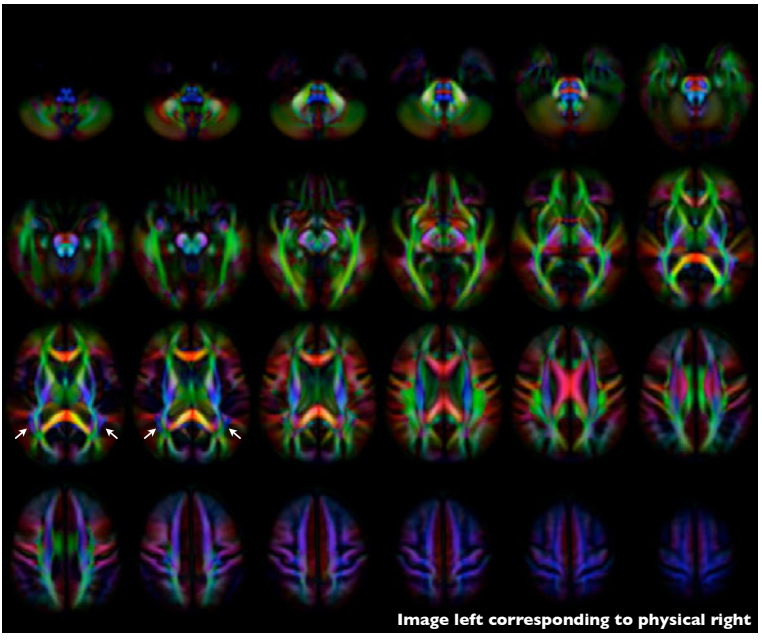

Fig. 1. Axial slices of the fiber orientation map of the constructed DTI template. The fiber orientations are visualized with the standard RGB encoding: red for left-right, green for anterior-posterior and blue for inferior-superior. The two pairs of white arrows highlight the visually distinct asymmetry in the left and right SLFs.

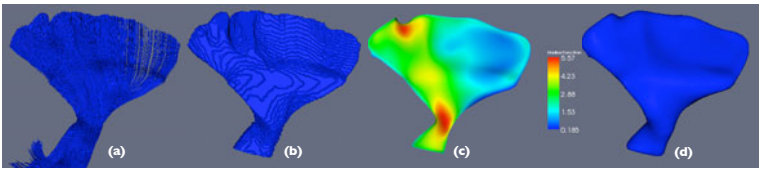

Fig. 2. The surface-based geometric modeling of the left CST. Panel (a): The results from fiber tractography. Panel (b): The binary segmentation computed from the fiber tracking results. Panel (c): The skeleton surface of the cm-rep model fitted to the binary segmenation overlaid with the corresponding radius function. Panel (d): The boundary surface corresponding to the fitted cm-rep model.

The result of applying the surface-based tract models to identify WM changes in ALS is shown in Fig. 4. Under the stringent significance level described in Sec. 2.5, we found three significant clusters of reduced FA in ALS compared to healthy controls. This finding is highly consistent with that of our previous analysis of this dataset using the same analysis [omitted]. The previous analysis reported two significant clusters, one on each CST, in the similar location as the

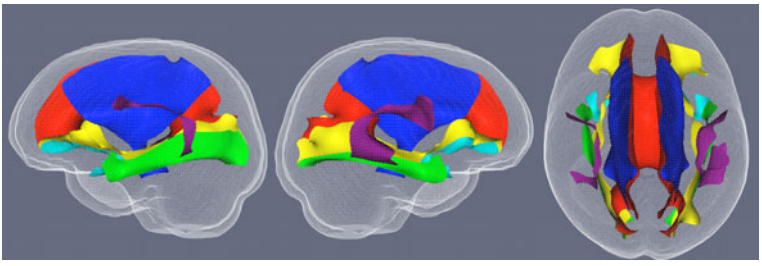

Fig. 3. The skeleton surfaces of the cm-rep models fitted to all the tracts. The skeleton surface of CC is colored in red. The surfaces of left and right CSTs, IFOs, ILFs, SLFs and UNCs are colored in blue, yellow, green and cyan, respectively. The brain mask is also shown as a translucent mesh for anatomical guidance. From left to right are the views of the skeleton surfaces from left (physical right), right (physical left), and top.

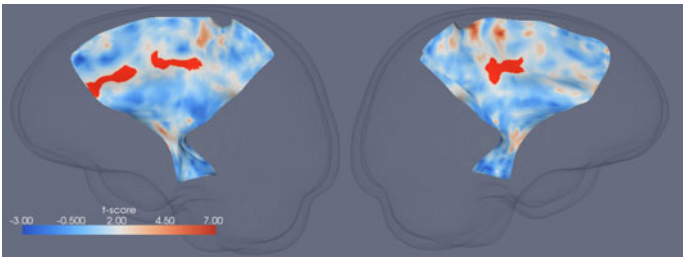

Fig. 4. The significant clusters of reduced FA in ALS compared to healthy controls (in red) overlaid on the skeleton surfaces of the CSTs. From left to right are the right and left CSTs.

ones identified here. The cluster on the right CST covers the combined area of the two clusters on the right CST found here.

4 Discussion

In this paper, we described the construction of a population-specific DTI template for the aging population. The template will enable standard whole-brain analyses, such as the popular TBSS method [2], to leverage advanced tensor-based spatial normalization techniques. Equipped with the parcellation of a large set of major WM tracts and their corresponding skeleton surface models, it will also support the recent development in tract-specific analysis by Yushkevich et al. [3]. We demonstrated qualitatively the feasibility of using the template for analyzing data acquired with different scanners or diffusion protocols, which should encourage its adoption as a useful public resource for the broad neuroimaging community studying aging and aging-related diseases.

Acknowledgment. The authors gratefully acknowledge support of this work by the NIH via grants AG027785 (PY), DA022807 (JG), EB006266 (JG), EB009321 (JG), NS061111 (PY), and NS065347 (JG).

References

1. Pierpaoli, C., Jezzard, P., Basser, P.J., Barnett, A., Chiro, G.D.: Diffusion tensor MR imaging of the human brain. Radiology 201 (1996)
2. Smith, S.M., Jenkinson, M., Johansen-Berg, H., Rueckert, D., Nichols, T.E., Mackay, C.E., Watkins, K.E., Ciccarelli, O., Cader, M.Z., Matthews, P.M., Behrens, T.E.J.: Tract-based spatial statistics: Voxelwise analysis of multi-subject diffusion data. NeuroImage 31 (2006)
3. Yushkevich, P.A., Zhang, H., Simon, T.J., Gee, J.C.: Structure-specific statistical mapping of white matter tracts. NeuroImage 41, 448–461 (2008)
4. Zhang, H., Avants, B.B., Yushkevich, P.A., Woo, J.H., Wang, S., McCluskey, L.F., Elman, L.B., Melhem, E.R., Gee, J.C.: High-dimensional spatial normalization of diffusion tensor images improves the detection of white matter differences in amyotrophic lateral sclerosis. TMI 26, 1585–1597 (2007)
5. Mori, S., Oishi, K., Jiang, H., Jiang, L., Li, X., Akhter, K., Hua, K., Faria, A.V., Mahmood, A., Woods, R., Toga, A.W., Pike, G.B., Neto, P.R., Evans, A., Zhang, J., Huang, H., Miller, M.I., van Zijl, P., Mazziotta, J.: Stereotaxic white matter atlas based on diffusion tensor imaging in an icbm template. NeuroImage 40, 570–582 (2008)
6. Arsigny, V., Fillard, P., Pennec, X., Ayache, N.: Log-Euclidean metrics for fast and simple calculus on diffusion tensors. MRM 56, 411–421 (2006)
7. Guimond, A., Meunier, J., Thirion, J.P.: Average brain models: a convergence study. CVIU 77, 192–210 (2000)
8. Zhang, H., Yushkevich, P.A., Alexander, D.C., Gee, J.C.: Deformable registration of diffusion tensor MR images with explicit orientation optimization. MIA 10 (2006)
9. Alexander, D.C., Pierpaoli, C., Basser, P.J., Gee, J.C.: Spatial transformations of diffusion tensor magnetic resonance images. TMI 20 (2001)
10. Wakana, S., Jiang, H., Nagae-Poetscher, L.M., van Zijl, P.C., Mori, S.: Fiber tract-based atlas of human white matter anatomy. Radiology 230 (2004)
11. Lawes, I.N., Barrick, T.R., Murugam, V., Spierings, N., Evans, D.R., Song, M., Clark, C.A.: Atlas-based segmentation of white matter tracts of the human brain using diffusion tensor tractography and comparison with classical dissection. NeuroImage 39 (2008)
12. Yushkevich, P.A., Piven, J., Hazlett, H.C., Smith, R.G., Ho, S., Gee, J.C., Gerig, G.: User-guided 3D active contour segmentation of anatomical structures: significantly improved efficiency and reliability. NeuroImage 31, 1116–1128 (2006)
13. Lazar, M., Field, A.S., Lee, J., Alexander, A.L.: Lateral asymmetry of superior longitudinal fasciculus: a white matter tractography study. In: ISMRM (2004)